22. Krall JM, Uthoff VA, Harley JB. A step-up procedure for selecting variables associated with survival. *Biometrics* 1975; 31: 49–57
23. Germain DP, Waldek S, Banikazemi M *et al.* Sustained, long-term renal stabilization after 54 months of agalsidase beta therapy in patients with Fabry disease. *J Am Soc Nephrol* 2007; 18: 1547–1557
24. Weidemann F, Niemann M, Breuning F *et al.* Long-term effects of enzyme replacement therapy on Fabry cardiomyography: evidence for a better outcome with early treatment. *Circulation* 2009; 119: 524–529
25. Feriozzi S, Torras J, Cybulla M *et al.* The effectiveness of long-term agalsidase alfa therapy in the treatment of Fabry nephropathy. *J Am Soc Nephrol* 2012; 7: 60–69
26. Skrunes R, Svarstad E, Kampevold Larsen K *et al.* Reaccumulation of globotriaosylceramide in podocytes after agalsidase dose reduction in young Fabry patients. *Nephrol Dial Transplant* 2017; 32: 807–813
27. Wu JC, Ho CY, Skali H *et al.* Cardiovascular manifestations of Fabry disease: relationship between left ventricular hypertrophy, disease severity, and alpha-galactosidase A activity. *Eur Heart J* 2010; 31: 1088–1097
28. Kampmann C, Linhart A, Baehner F *et al.* Onset and progression of the Anderson-Fabry disease related cardiomyopathy. *Int J Cardiol* 2008; 130: 367–373
29. Warnock DG, Ortiz A, Mauer M *et al.* Renal outcomes of agalsidase beta treatment for Fabry disease: role of proteinuria and timing or treatment initiation. *Nephrol Dial Transplant* 2012; 27: 1042–1049
30. Warnock DG, Thomas CP, Vujkovac B *et al.* Antiproteinuric therapy and Fabry nephropathy: factors associated with preserved kidney function during agalsidase-beta therapy. *J Med Genet* 2015; 52: 860–866
31. Kleiner J, Dehout F, Schwarting A *et al.* Prevalence of uncontrolled hypertension in patients with Fabry disease. *Am J Hypertens* 2006; 19: 782–787
32. Ortiz A, Oliveira JP, Waldek S *et al.* Nephropathy in males and females with Fabry disease: cross-sectional description of patients before treatment with enzyme replacement therapy. *Nephrol Dial Transplant* 2008; 23: 1600–1607
33. 2013 ESH/ESC guidelines for the management of arterial hypertension: The task force for the management of arterial hypertension of the European Society of Hypertension (ESH) and of the European Society of Cardiology (ESC). *J Hypertens* 2013; 31: 1281–1357
34. Schieppati A, Remuzzi G. Proteinuria and its consequences in renal disease. *Acta Paediatr Suppl* 2003; 92: 9–13
35. Ortiz A, Abiose A, Bichet DG *et al.* Time to treatment benefit for adult patients with Fabry disease receiving agalsidase β: data from the Fabry Registry. *J Med Genet* 2016; 53: 495–502
36. Biegstraaten M, Arngrimsson R, Barbey F *et al.* Recommendations for initiation and cessation of enzyme replacement therapy in patients with Fabry disease: the European Fabry Working Group consensus document. *Orphanet J Rare Dis* 2015; 10: 36

Received: 10.5.2016; Editorial decision: 10.8.2016

Nephrol Dial Transplant (2017) 32: 2097–2105
doi: 10.1093/ndt/gfw362
Advance Access publication 17 October 2016

ORIGINAL ARTICLE

Reduction of cortical oxygenation in chronic kidney disease: evidence obtained with a new analysis method of blood oxygenation level-dependent magnetic resonance imaging

Bastien Milani[1,2], Annalisa Ansaloni[1], Sofia Sousa-Guimaraes[1], Nima Vakilzadeh[1], Maciej Piskunowicz[3], Bruno Vogt[4], Matthias Stuber[2,5], Michel Burnier[1] and Menno Pruijm[1]

[1]Service of Nephrology and Hypertension, CHUV, Lausanne, Switzerland, [2]Center for Biomedical Imaging, University Hospital Lausanne, Lausanne, Switzerland, [3]Department of Radiology, Medical University of Gdansk, Gdansk, Poland, [4]Service of Nephrology and Hypertension, Bern University Hospital, Bern, Switzerland and [5]Department of Radiology, CHUV, Lausanne, Switzerland

Correspondence and offprint requests to: Menno Pruijm; E-mail: menno.pruijm@chuv.ch

ABSTRACT

Background. Determinations of renal oxygenation by blood oxygenation level-dependent magnetic resonance imaging (BOLD-MRI) in chronic kidney disease (CKD) patients have given heterogeneous results, possibly due to the lack of a reproducible method to analyse BOLD-MRI. It therefore remains uncertain whether patients with CKD have a reduced renal tissue oxygenation. We developed a new method to analyse BOLD-MRI signals and applied it to CKD patients and controls.

Methods. MRI was performed under standardized conditions before and 15 min after IV furosemide in 104 CKD patients, 61 hypertensives and 42 controls. MR images were analysed with the new twelve-layer concentric objects method (TLCO) that divides renal parenchyma in 12 layers of equal thickness. The mean R2* value of each layer was reported, along with the change in R2* between successive layers, as measured by the slope steepness of the relevant curve.

Results. Inter-observer variability was 2.3 ± 0.9%, 1.9 ± 0.8% and 3.0 ± 2.3% in, respectively, controls, moderate and severe CKD. The mean R2* of the outer (more cortical) layers was significantly higher in CKD, suggesting lower cortical oxygenation as compared with controls. In CKD patients, the response to furosemide was blunted in the inner (more medullary) layers, and the R2* slope was flatter. In multivariable regression analysis, the R2* slope correlated positively with estimated glomerular filtration rate (eGFR) in patients with an eGFR <90 mL/min/1.73 m^2 ($P < 0.001$).

Conclusions. Using the new TLCO method, we confirm the hypothesis that renal cortical oxygenation is reduced in CKD in humans, and that the level of cortical oxygenation correlates with CKD severity.

Keywords: blood oxygen level-dependent MRI, chronic kidney disease, furosemide, renal tissue oxygenation, twelve-layer concentric objects (TLCO) technique

INTRODUCTION

Chronic kidney disease (CKD) has become a major public health problem with a global prevalence in the general population of ∼10% [1]. Renal hypoxia may play a role in the development and progression of CKD, as proposed by the chronic hypoxia model [2]. Animal studies measuring intra-renal pO_2 with microelectrodes have supported this hypothesis [3, 4]. In humans, blood oxygenation level-dependent magnetic resonance imaging (BOLD-MRI) offers the possibility to measure tissue oxygenation non-invasively [5, 6]. Surprisingly, however, BOLD-MRI studies have not consistently found that there is renal tissue hypoxia in patients suffering from CKD [7–10]. Thus, the role of renal tissue hypoxia in the pathogenesis of CKD progression in humans remains uncertain. Animal studies have reported linear relationships between directly measured renal pO_2 values and R2* (i.e. the lower the tissue pO_2, the higher the R2*), thus supporting the hypothesis that BOLD-MRI measures tissue pO_2 with a reasonable accuracy [5, 11–14]. Therefore, the uncertainty may be partly related to the methods used to analyse BOLD-MRI data. We have previously shown that the classical region of interest (ROI) technique, based on manual placement of circle-shaped ROIs in the cortex and medulla, has a high inter-observer variability in CKD due to loss of cortico-medullary differentiation [15]. In that same article, we proposed a new semi-automatic technique, called 'concentric objects' (CO) or onion peel technique. This technique divides the kidney parenchyma in six layers of equal thickness and reports the mean R2* value of each layer. Notably, the CO technique had very low inter-observer variability. When applied to a small number of subjects, it also suggested that R2* values in the outer layers were higher in CKD patients as compared with healthy controls. However, cysts had to be suppressed manually, the technique could not be applied to non-oval-shaped kidneys and the relatively limited number of layers lacked precision. Finally, the CO technique only reported the mean R2* values of each layer, without analysing the relative changes in mean R2* from superficial to deeper layers of the renal parenchyma. We have therefore improved the technique by developing an automated, twelve-layer CO technique (called the TLCO technique) to analyse BOLD images. In this article, we describe this new technique and provide data on its inter-observer reproducibility. Based on a large cohort, we have also assessed whether there are indeed differences in R2* values between CKD patients as compared with normotensive and hypertensive controls.

MATERIALS AND METHODS

Participants

All the individuals included in this study are part of the LauBOLD cohort. LauBOLD is a cohort evaluating the prognostic value of renal tissue oxygenation on the progression of kidney diseases, as previously described in more detail [7]. In brief, adult patients with CKD stages 1–5, irrespective of cause, were recruited at our nephrology outpatient clinic, as well as hypertensive individuals without CKD. CKD was defined as the presence of structural kidney damage, an estimated glomerular filtration rate (eGFR) <60 mL/min/1.73 m^2 or albuminuria >300 mg/24 h for at least 3 months [16]. The following criteria applied to healthy volunteers: no drug intake, absence of kidney abnormalities at screening renal ultrasound, eGFR ≥60 mL/min/1.73 m^2 and absence of (micro) albuminuria or hypertension. MR scans were exclusively performed for this study, and not for medical reasons.

Reproducibility study. For this part of the study, 20 healthy controls, 18 CKD patients with mild to moderate CKD (eGFR ≥45 mL/min/1.73 m^2 according to the CKD-EPI formula) and 14 CKD patients with more severe CKD (eGFR <45 mL/min/1.73 m^2) were randomly selected from the LauBOLD cohort. Their scans were analysed by two experienced observers who were unaware of the CKD stage.

Comparison study. In the second part of the study, differences in R2* between CKD patients, hypertensives and normotensive controls were analysed in all participants of the LauBOLD cohort with BOLD images of sufficient quality (i.e. without substantial movement or other artefacts).

The study was approved by the local ethical committee (Ethical Committee of the Canton de Vaud, Switzerland) and written informed consent was obtained from all individuals.

Study visit

Every participant followed the same hydration protocol (water intake of 3 mL/kg at 8 a.m. at home, followed by 1 mL/kg/h on the day of the MRI exam). A 24 h urine collection on the day preceding the BOLD-MRI examination was performed to verify salt intake. All medication intake was continued on the day of the MRI exam. BOLD-MRI was performed between 1 and 2 p.m. All participants underwent a BOLD-MRI before and 15 min after the injection of 20 mg of furosemide (Lasix®, Sanofi-Aventis, Paris, France) during this time slot. No contrast agents were administered.

BOLD-MRI technique

BOLD-MRI measures R2* (defined as 1/T2*) for each voxel of a sample. The R2* is expressed in s^{-1} and is defined as the decay rate (1/decay time) of the transversal component of the macroscopic magnetization of the corresponding voxel, such that $M = M0\ e^{(-R2^{*}t)}$. This parameter is influenced by any kind of inhomogeneity in the local static magnetic field, in particular by the effect of deoxyhemoglobin, which has a strong positive magnetic susceptibility. The susceptibility difference between deoxyhemoglobin and surrounding tissues will generate intravoxel B-field inhomogeneities. As such, the decay rate R2* will be enhanced when the local deoxyhaemoglobin concentration is increased. This is the case when renal tissue oxygenation is low, assuming that blood pO_2 is in equilibrium with the surrounding tissue pO_2.

MR images were acquired using four coronal slices on a 3T-whole-body MR system (Magnetom Prisma, Siemens Medical Systems, Erlangen, Germany), as described previously [7]. Twelve T2*-weighted images were collected for each coronal slice within a single breath-hold of 16.6 seconds (in expiration) using a modified Multi Echo Data Image Combination sequence for BOLD analysis with the following parameters: repetition time 65 ms, echo time 6–52.2 ms (equidistant echo time spacing of 4.2 ms), radiofrequency excitation angle 30°, field of view 400 × 400 mm^2, voxel size 0.8 × 0.8 × 5 mm^3, slice thickness 5 mm, slice distance 5.5 mm, bandwidth 331 Hz/pixel and matrix 256 × 256 (interpolated to 512 × 512).

Analysis of images with the TLCO technique

The TLCO technique was implemented with Matlab 7.11 (The MathWorks Inc., Natick, MA, USA). R2* maps were calculated on a voxel by voxel basis, using a linear least squares fit of the logarithm of the signal. In each selected coronal slice, the circumference of the renal parenchyma was drawn manually. The outer and inner boundaries of the kidneys were visually identified by the investigator. After manual definition of the parenchyma, a locally programmed automatic algorithm divided the parenchyma into 12 concentric areas of equal thickness as shown in Figure 1. These areas were called the concentric objects (COs), each cover a set of pixels with a constant (range of) depth inside the kidney. In certain cases, air in the intestines created magnetic susceptibility artefacts. To account for this, large deviations from the fitted exponential were excluded from the analysis by applying a mask on the image that retained only the voxels for which the mean of the square of the relative errors between the fitted exponential and the data points were smaller than 10% (= 0.1). In addition, voxels with R2* values below 10 s^{-1} or above 50 s^{-1} were excluded, since these values are not in the range of significance for the renal parenchyma and most likely corresponded to cysts or artefacts. Concerning large cysts or tumours, the algorithm that draws the COs was programmed to neglect their presence (Figure 1).

The COs were also extended in three dimensions. The set of voxels present in one layer, and thus at a constant (range of) depth in the renal parenchyma of all (four) slices of the

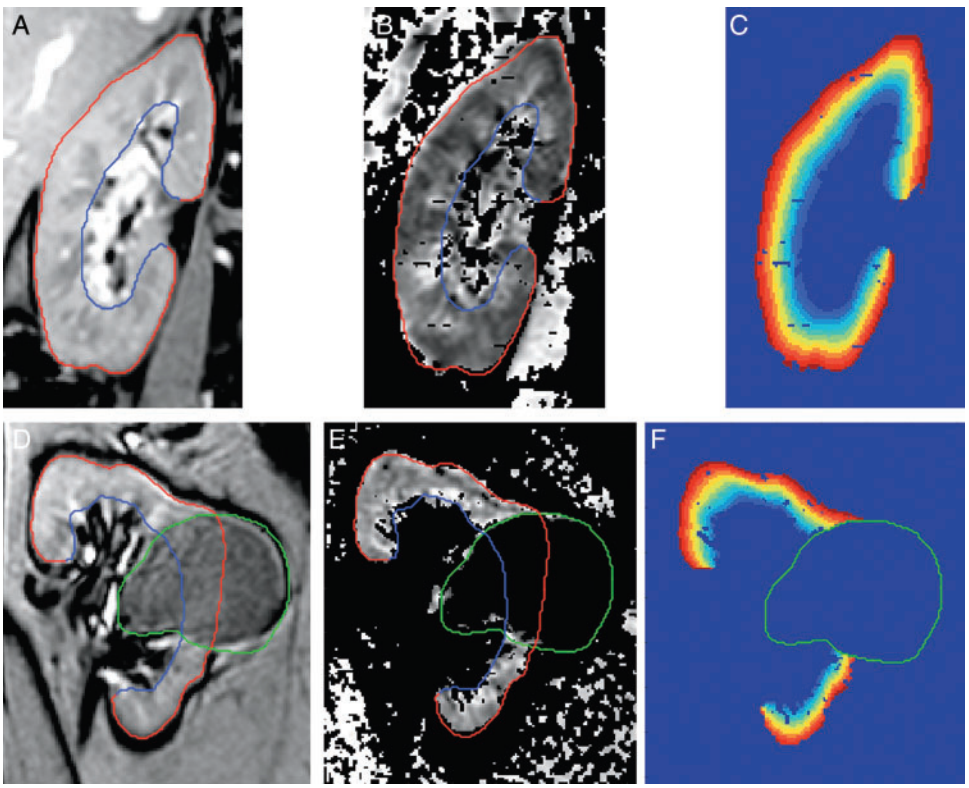

FIGURE 1: The TLCO technique. The outer border (in red) and inner border (in blue) of the renal parenchyma are drawn manually on anatomical templates (**A** and **D**); corresponding R2* maps are shown in the middle (**B** and **E**). After importation in Matlab, an automatic procedure divides the selected renal parenchyma into 12 layers of equal thickness (**C**); voxels with R2* <10 or >50 s^{-1} are suppressed, as well as voxels with badly exponential-fitted signal (dark blue dots). Cysts are also suppressed (**F**).

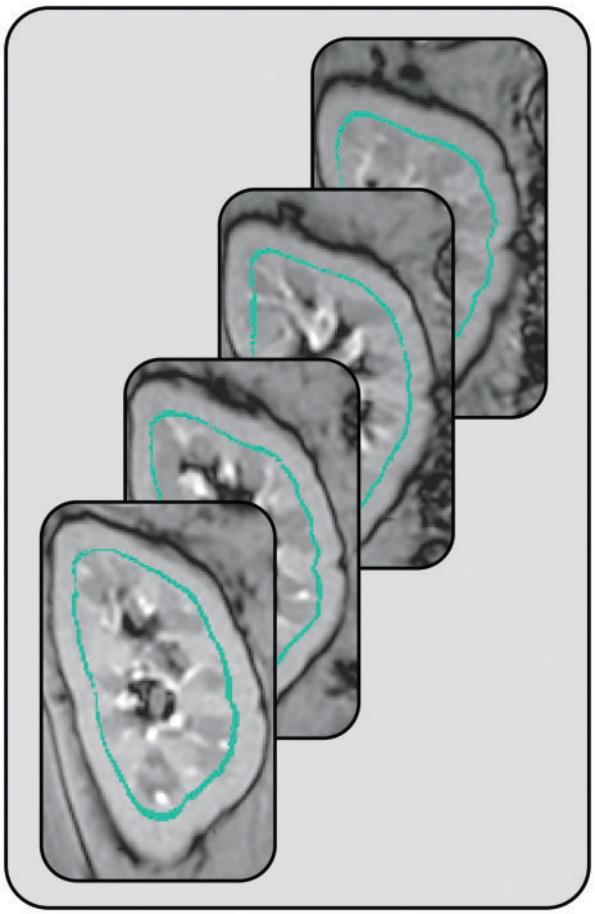

FIGURE 2: An example of one CO3D in a patient; a CO3D (12 per kidney) is the collection of voxels at equal relative depth (shown in the figure: eighth layer, between 58.3 and 66.7% of depth) of all four slices taken during a BOLD-MRI exam of the kidney.

kidney was called a CO3D (CO in 3 dimensions), as shown in Figure 2.

By averaging the R2* values in each of the 12 CO3Ds, the mean R2* of each layer was obtained. The mean R2* values of all 12 CO3Ds at increasing depth can be plotted as a curve, and was called the R2* radial profile (an example for one participant is shown in Figure 3A). The *x*-axis of this curve represents the percent of relative depth (ranging from 0% to 100%) and the *y*-axis represents the mean R2* of each CO3D. The superficial CO3Ds (cortex side) are shown on the left of the graph, with the inner CO3Ds (medulla side) on the right.

For each kidney, the R2* radial profile was calculated both before and 15 min after the injection of furosemide. A third curve, defined as the 'response profile', corresponded to the pre-furosemide curve minus the post-furosemide curve and represented the absolute furosemide-induced change in R2*, as a function of the depth (Figure 3B). A high difference corresponded to a large decrease of R2* and presumably an increase in oxygenation.

The shape and slope of the R2* radial profile

The radial R2* curves were almost always linear between its deepest point and the next four points to its right. Five points were therefore selected in order to measure the slope of the curve

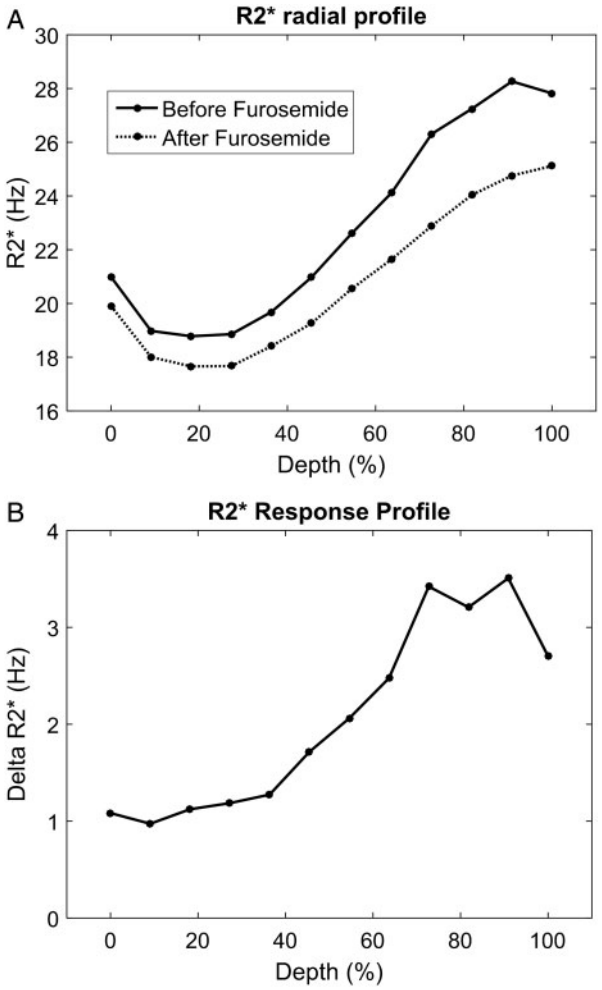

FIGURE 3: (**A**) Example of a curve connecting the mean R2* of the 12 layers (CO3Ds) of both kidneys in a normotensive participant, called the R2* radial profile. The R2* radial profile is shown before and after the administration of furosemide. (**B**) Example of the absolute furosemide-induced change in R2* layer by layer in the same participant, called R2* response profile. The largest change in R2* is seen in the deeper layers, corresponding to mainly medullary tissue.

within this linear section: the minimum of the radial profile and the four next points to its right. The R2* radial profiles were shifted down to the *x*-axis, such that the value of the third point was 0 for every curve. This shift permitted a comparison of the shapes of the curves, instead of their absolutes values (Supplementary data, Figure S1). In this way, the change in R2* from superficial to profound layers could be compared, independently of its absolute values. The larger the difference in R2* between the lowest and highest point of the shifted R2* profile, the steeper the slope, and thus the larger the presumed oxygenation difference between outer (more cortical) and inner (mainly medullary) layers. The slope of each kidney R2* profile was expressed as the change in Hertz per percentage change of depth.

Statistical analysis

Statistical analysis was performed with STATA 12.0 (StataCorp, College Station, TX, USA). Quantitative values were

expressed as mean ± standard deviation or median values (range), as appropriate. Normality was first assessed graphically (histograms), and then numerically with skewness and kurtosis tests. Qualitative variables were expressed as number (percentage). ANOVA, Student's *t* test, Wilcoxon ranksum test or χ^2 test were used as appropriate to compare clinical characteristics and R2* values of the groups.

R2* values of each of 12 layers of the kidneys were analysed separately by group (control, CKD 1–3a and CKD 3b–5). The coefficient of variation, Lin's correlation coefficient and Blant–Altman curves were used to assess inter-observer variability of the mean R2* values of each layer (CO3D), and of each curve (see Supplementary data for more details).

In the comparison study, between-group differences of R2* values were compared using two-tailed *t*-tests.

The regression coefficient β of the R2* slope of each kidney was calculated with the linear least square regression technique; assumptions were checked for this model. In order to study the relationship between the slope and eGFR, the mean slope of each individual was calculated, with the presumption that eGFR represents the sum of the filtration rate of both kidneys. Multivariate linear regression analysis was performed to explore the associations of clinical variables with the R2* slope (dependent variable). Unadjusted analyses were performed first, followed by multivariable analyses integrating all variables associated with the slope in unadjusted analysis. We further explored the association of the R2* slope with eGFR, by stratifying eGFR in groups of either <90 or ≥90 mL/min/1.73 m^2. This was performed due to the relationship between R2* slope and eGFR not being purely linear, with a visually observed change in the approximate slope at ∼90 mL/min/1.73 m^2. For all analyses, a P-value <0.05 was considered as significant.

RESULTS

Inter-observer variability study

Clinical and laboratory characteristics of the 52 individuals who participated in this part of the study are shown in Table 1. For the TLCO technique, a low inter-observer variability was found, with mean coefficients of variation (CVs) of 2.2 ± 1.5, 2.0 ± 1.7 and 3.1 ± 2.9%, respectively, in the healthy, mild CKD and severe CKD groups (Table 2). Lin's correlation coefficient was systematically above 85%, except for the two deepest layers. Similar results were found after furosemide (Supplementary data, Table S1).

Regarding the variability of the slope of the R2* curve, the mean CV varied between 15.9 and 26.8%, and Lin's correlation coefficient between 78 and 80% in the three groups (Table 2). The Bland–Altman plot of the measured slopes is shown in Supplementary data, Figure S2. The mean difference of the slopes between both observers was 0.0033 s^{-1}/(% of depth) and was not significant (P = 0.1).

Comparison study

Of the 214 LauBOLD participants, seven were excluded due to poor image quality. Clinical characteristics of the remaining 207 participants are shown in Table 1. Details on drug intake are provided in Supplementary data, Table S2.

The radial R2* profiles of the control, hypertensive and CKD groups of the entire LauBOLD cohort are shown in Figure 4. There was no significant difference between the normotensive and the hypertensive control group in the R2* values of any of the 12 layers. However, the mean R2* of the outer layers of the CKD group was significantly higher than hypertensive and normotensive controls, suggesting lower oxygenation, whereas R2*

Table 1. Clinical characteristics of participants in the reproducibility study (left columns) and the entire LauBOLD cohort (right columns)

	Reproducibility study			Entire LauBOLD cohort		
	Control	CKD 1–3a	CKD 3b–5	Control	Hypertensive	CKD
Number of participants	20	18	14	42	61	104
Age (years)	47 ± 10	50 ± 9	68 ± 9[a]	46 ± 13	56 ± 12	56 ± 15[b]
Sex (% female)	50	50	50	52.4	36.1	31.7[b]
Diabetes (%)	0	28	43	0	16.4[c]	35.0[b]
Cause of CKD (%)						
Diabetes		27.8	42.8			35.0
Hypertension		27.8	25.7			30.1
Glomerulonephritis		16.7	14.3			22.8
Other		21.7	17.2			12.1
Creatinine (µmol/L)	76 ± 15	101 ± 35[a]	221 ± 78[a]	74 ± 14	75 ± 12[c]	151 ± 91[b]
eGFR (mL/min/1.73 m^2)	95 ± 13	72 ± 27[a]	25 ± 9[a]	97 ± 14	92 ± 16[c]	56 ± 30[b]
Body mass index (kg/m^2)	28 ± 5	29 ± 4	29 ± 5	26 ± 5	28 ± 5	28 ± 4
Systolic BP (mmHg)	120 ± 12	134 ± 16[a]	137 ± 23[a]	124 ± 14	142 ± 16	134 ± 19[b]
Diastolic BP (mmHg)	75 ± 10	82 ± 10[a]	71 ± 13	76 ± 12	82 ± 10[c]	76 ± 11
Urinary 24 h volume (L)	2.2 ± 1.2	2.4 (1.6; 2.9)	2.3 (1.6; 2.7)	2.1 (1.6; 2.7)	1.8 (1.4; 2.5)	1.8 (1.3; 2.7)
Urinary 24 h sodium (mmol)	178 ± 82	182 ± 104	151 ± 61	159 ± 73	179 ± 79	169 ± 85
Haemoglobin (g/dL)	135 ± 11	133 ± 16	116 ± 12[a]	136 ± 11	138 ± 13[c]	130 ± 18
Hematocrit (%)	40 ± 3	40 ± 5	35 ± 3[a]	40 ± 3	40 ± 3[c]	38 ± 5
Glycaemia (mmol/L)	5.8 ± 1.6	6.9 ± 3.2	7.8 ± 3.8[a]	5.6 ± 1.0	6.1 ± 1.2	6.6 ± 2.4[b]

Values are expressed as mean ± standard deviation, median (25; 75th percentile) or as a percentage. BP, blood pressure.
[a]P < 0.05 with respect to the two sided *t*-test, Wilcoxon ranksum test or χ^2 test between moderate CKD or advanced CKD versus controls in the reproducibility study.
[b]CKD versus controls in the entire LauBOLD cohort.
[c]Hypertensives versus CKD in the entire LauBOLD cohort.

Table 2. Inter-observer variability of the TLCO technique expressed as coefficient of variation (in %) and correlation coefficient of each of 12 separate layers, according to group

	Coefficient of variation			Correlation coefficient of Lin		
	Control	CKD 1–3a	CKD 3b–5	Control	CKD 1–3a	CKD 3b–5
Curves	2.3 ± 0.9	1.9 ± 0.8	3.0 ± 2.3	96.2 ± 2.4	94.4 ± 7.4	87.1 ± 13.4
CO 1	1.8 ± 1.5	2.7 ± 2.4	3.8 ± 3.0	98.4	93.3	86.5
CO 2	1.3 ± 0.9	1.6 ± 1.2	2.7 ± 2.2	99.3	98.4	93.5
CO 3	1.2 ± 1.0	1.3 ± 1.4	2.4 ± 2.4	99.2	98.2	94.4
CO 4	1.4 ± 1.3	1.0 ± 0.8	1.7 ± 1.6	98.6	99.2	97.5
CO 5	1.9 ± 1.3	1.3 ± 1.0	1.9 ± 1.5	97.6	98.6	97.4
CO 6	1.9 ± 1.3	1.6 ± 1.4	1.6 ± 1.4	97.2	97.0	97.9
CO 7	1.9 ± 1.3	1.6 ± 1.3	2.5 ± 2.3	96.9	96.8	94.2
CO 8	2.2 ± 1.6	2.1 ± 1.7	2.9 ± 3.2	95.2	93.2	89.7
CO 9	2.8 ± 2.0	2.2 ± 2.0	3.0 ± 3.8	91.8	91.5	85.4
CO 10	3.2 ± 2.0	2.6 ± 1.7	4.0 ± 4.1	90.6	91.3	78.8
CO 11	3.3 ± 2.4	2.6 ± 2.2	4.4 ± 4.5	88.2	86.2	72.5
CO 12	3.7 ± 2.2	3.6 ± 3.6	6.6 ± 6.3	85.5	70.2	57.0
Slope	15.9 ± 12.7	22.8 ± 16.2	26.8 ± 29.3	78.2	78.5	80.3

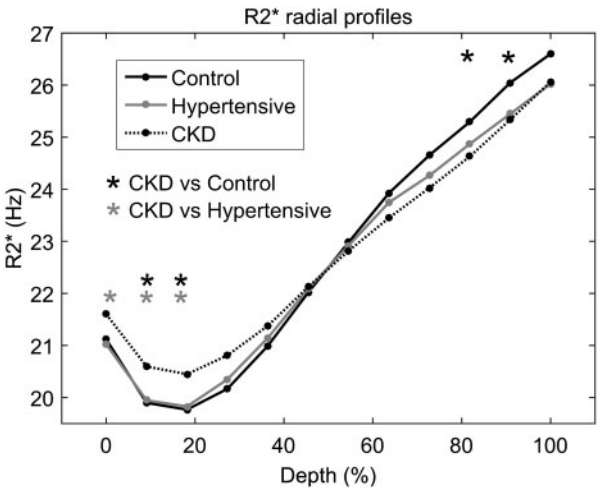

FIGURE 4: Averaged R2* radial profiles of all normotensive controls, hypertensive controls and patients with CKD. R2* values of the outer layers were significantly higher in the CKD group, suggesting lower cortical oxygenation, whereas R2* values of the inner layers were higher in normotensive controls as compared with CKD patients. Student's *t*-tests were used to compare R2* values of each layer; *P < 0.05.

values of layer 10 and 11 were significantly lower than normotensive controls. Absolute furosemide-induced changes in R2* were significantly smaller in CKD patients as compared with hyper- or normotensive controls (Figure 5).

Shifted R2* profiles (i.e. shifting down to the *x*-axis of the R2* profile, such that the point with the lowest R2* value was 0 for every curve and only relative differences are identified) are shown in Figure 6 according to four eGFR categories, for all LauBOLD participants taken together. In all categories, R2* increased at increasing depth, suggesting lower oxygenation in more medullary zones. The increase in R2* was highest in members of the highest eGFR category. The corresponding R2* slope was therefore the steepest in the highest eGFR category, with the slopes of the four categories being 0.032, 0.047, 0.070 and 0.088 s^{-1}/depth percentage (P-value for trend < 0.001). The slope was less steep in CKD patients as compared with hyper or normotensive controls (Supplementary data, Figure S3).

The continuous association between the radial profile-slope and the eGFR, with all groups combined, is graphically illustrated in Figure 7.

In univariate linear regression analysis, the clinical variables of female gender, eGFR and haemoglobin were positively associated with the R2* slope (outcome variable), whereas age, having diabetes and the daily intake of angiotensin 2 receptor blockers ($n = 66$) or thiazide diuretics ($n = 37$) were negatively associated with the R2* slope (Table 3). The number of patients taking daily loop diuretics was low ($n = 19$), and this variable was therefore not included in the model. In multivariate analysis, adjusted for all variables that reached a P-value <0.10 in univariate analysis, only eGFR and female gender remained (positively) associated with the R2* slope, whereas chronic thiazide diuretic intake correlated negatively.

Graphically, the relationship between the R2* slope and eGFR was not linear, with a change in slope at an eGFR around 90 mL/min/1.73 m^2. We therefore also stratified the analysis by eGFR ≥90 and <90 mL/min/1.73 m^2. There was indeed a significant and positive association between the eGFR and the slope (Pearson correlation coefficient 0.50, P < 0.001) when the eGFR was <90 mL/min/1.73 m^2 [regression coefficient β 0.059, 95% confidence interval (CI): 0.04 to 0.08, P < 0.001], but not ≥90 (β −0.021, 95% CI: −0.11 to 0.07, P = 0.63).

DISCUSSION

Taken together, the present study shows that the inter-observer variability of the new TLCO method is small, indicating that it is largely observer-independent, even in cases of severe CKD. In addition, we demonstrate that the R2* profiles obtained with this technique differ significantly between CKD patients and hypertensive or healthy controls. R2* values of the outer (more cortical) layers are significantly higher in CKD patients, suggesting a lower cortical oxygenation. Furosemide-induced changes

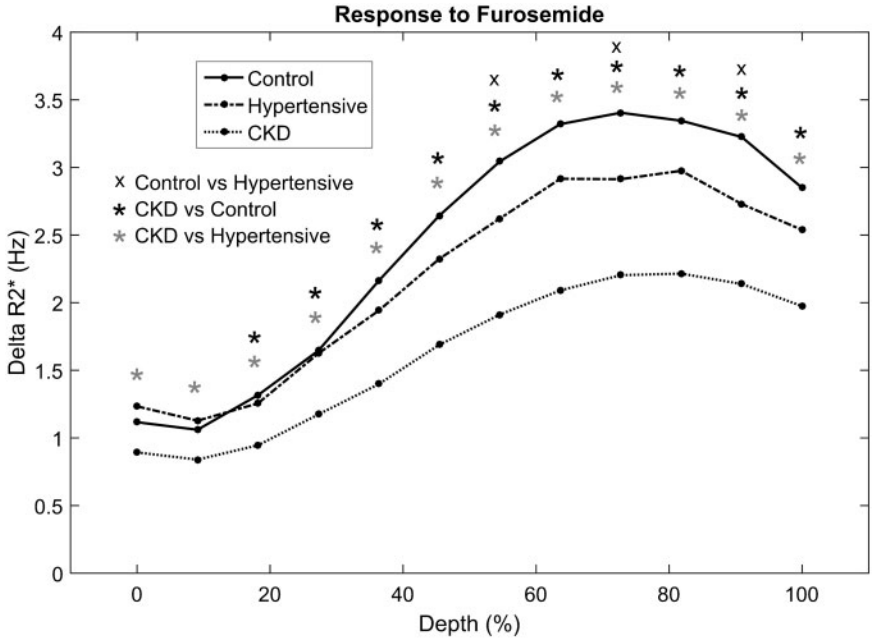

FIGURE 5: Absolute furosemide-induced changes in R2* (R2* profile), according to group.

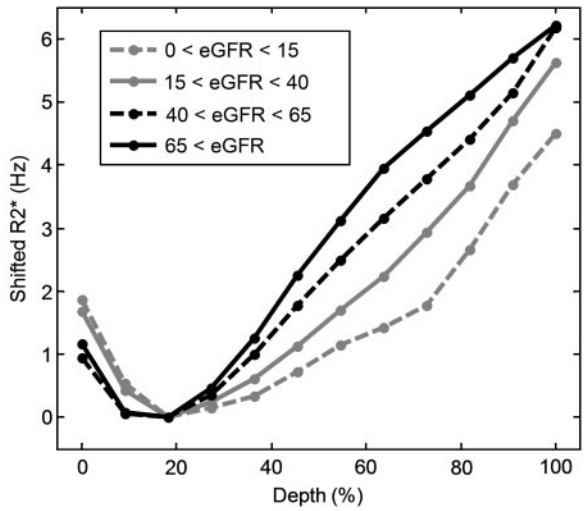

FIGURE 6: Shifted R2* radial profile at decreasing levels of eGFR, for all LauBOLD participants taken together. The largest increase in R2* over layers at increasing depth (corresponding to the steepest slope) was seen in the highest eGFR category, suggesting that the change in oxygenation from cortex to medulla was the largest in the highest eGFR group.

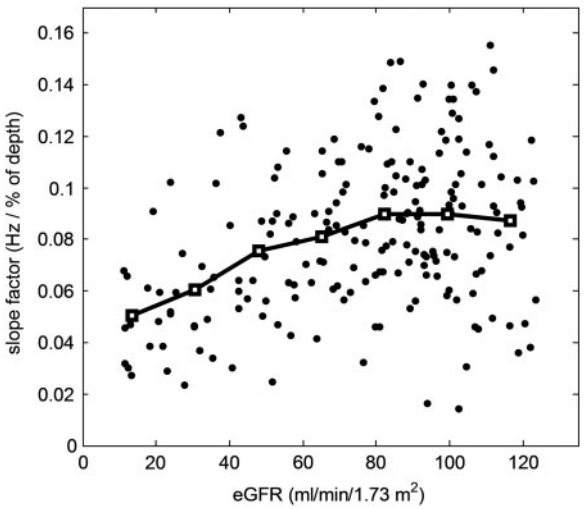

FIGURE 7: Mean slope factor across different levels of eGFR. The higher the eGFR, the higher the slope factor. A plateau of the slope factor was reached above 90 mL/min/1.73 m^2.

in R2* are also highly reproducible, and can be analysed layer-by-layer. In our cohort, smaller furosemide-induced changes are observed in the CKD group, especially in the deeper layers, indicating a lower furosemide-induced change in active sodium transport as compared with healthy or hypertensive participants. Finally, a new concept that takes into account the rate of change in R2* (the slope) from the outer to the inner border of renal parenchyma is introduced to analyse BOLD-MRI results. This analysis is less reproducible, but shows that the slope correlates strongly and positively with the eGFR, such that the higher the eGFR, the steeper the slope of the associated R2* change.

A multitude of techniques have been used to analyse BOLD-MRI to date, yet all have specific shortcomings. For instance, the fractional tissue hypoxia-method reports the percentage of R2* values above 30 s^{-1} [17]. This is an arbitrary threshold that cannot be applied to scanners of different field strengths or different populations. The compartmental method assumes that the R2* voxels follow a more Gaussian distribution in the cortex, and a gamma distribution in the medulla. Based on this assumption, an algorithm has been developed to decide whether a voxel belongs to the cortex or medulla [18]. However, this

Table 3. Clinical variables associated with the R2* slope factor (dependent variable) in uni- and multivariable regression analysis

	Unadjusted β (95% CI)	P	Adjusted β (95% CI)[a]	P
Age (per year)	−0.028 (−0.057; 0.002)	0.064	0.022 (−0.009; 0.053)	0.17
Sex (female versus male)	1.41 (0.56; 2.25)	0.001	1.59 (0.69; 2.49)	*0.001*
Body mass index (per kg/m^2)	0.0047 (−0.083; 0.093)	0.92	–	
Diabetes (yes versus no)	−1.21 (−2.34; −0.85)	0.035	0.22 (−0.92; 1.34)	0.71
Chronic thiazide diuretic intake (yes versus no)	−1.41 (−2.51; −0.31)	0.012	−1.22 (−2.28; −1.63)	*0.024*
Chronic ACE-inhibitor intake (yes versus no)	0.20 (−1.01; 1.41)	0.75	–	
eGFR (per mL/min/1.73 m^2)	0.038 (0.024; 0.051)	0.000	0.030 (0.013; 0.048)	*0.001*
Haemoglobin (per g/dL)	0.033 (0.006; 0.059)	0.015	0.031 (−0.002; 0.063)	0.06
Urinary 24 h sodium excretion (per mmol/day)	0.0004 (−0.005; 0.006)	0.88	–	

Values in italic: P <0.05.

[a]Multivariable regression analysis, adjusted for all variables with P < 0.1 in unadjusted analysis. Results are expressed as regression coefficient β (95% CI). ACE, angiotensin-converting enzyme.

algorithm depends on the absolute values of R2*, and to date, it is uncertain whether this algorithm is reliable in CKD. The classical ROI technique remains the most frequently used analytic approach of BOLD-MRI images, yet this method is prone to subjectivity in individuals with poor cortico-medullary differentiation [15]. Recently, Thacker *et al.* used large cortical ROIs and the entire renal parenchyma to analyse BOLD images; the method has a high inter-observer agreement, but does not provide detailed layer by layer information as obtained with the TLCO technique [19].

The lack of consensus on how to analyse BOLD-MRI images is probably one of the reasons that BOLD-MRI has not been regularly used in clinical practice. Therefore, a widely accepted procedure is needed. In our opinion, the TLCO technique overcomes most of the limitations mentioned above. Firstly, the TLCO technique is largely observer-independent, as demonstrated in this study. Secondly, the technique takes into account almost the entire surface of the renal parenchyma, and integrates geometrical information. Hence, the method is more sensitive to small differences in R2* than the ROI technique. This is illustrated in our study by the fact that the R2* levels of the outer layers were higher (suggesting lower oxygenation) in CKD patients than controls. These results are in contrast to a previous study that also included participants to the LauBOLD cohort but used the ROI technique, in which no difference in R2* was found between CKD patients, normo- and hypertensive controls [7]. Thirdly, the TLCO technique provides unique information on the renal response to external stimuli at different renal depths. This technique is therefore a powerful tool to study the effects of medication on renal oxygenation as estimated with BOLD-MRI [20]. The response to furosemide illustrates this potential. As expected, smaller decreases in R2* in response to furosemide were found in the CKD group. This is generally attributed to the lower change in furosemide-induced oxygen-consuming active sodium transport in CKD patients due to a reduced number of functioning nephrons [7, 21].

Quantitative analysis of BOLD-MRI remains limited due to lack of direct validation with oxygen sensors in humans. Additionally, R2* values are influenced by multiple external and internal factors such as hydration status [22], dietary sodium intake [23], and changes in vascular and tubular volume fraction [24]. A method that focuses less on the mean R2* values and more on its intra-compartmental distribution can overcome this limitation. As such, the analysis of the R2* slope offers a new way to analyse relative intra-kidney differences in R2* values. We observed that the radial R2* curves increased linearly between the third and seventh layer, suggesting a sharp decrease in oxygenation at this point, as previously reported in animal studies [4, 25, 26]. By offsetting the R2* value of the deepest point of the curve (in general at the third layer) to 0, the slope of this linear part can be assessed, and expressed as regression coefficient β, corresponding to the change in s^{-1} per percentage change of depth.

The slope of this linear fraction was flatter in CKD patients, and correlated strongly and positively with an eGFR below <90 mL/min/1.73 m^2, but not in cases when eGFR was ≥90 mL/min/1.73 m^2. This may possibly be explained as follows: in healthy kidneys, there is a large difference between cortical (high) and medullary (low) oxygenation, likely due to the high degree of oxygen-consuming active transport in the medulla. In CKD, cortical ischaemia increases, whereas active transport decreases in the medulla due to lack of functional tubuli, leading to a smaller difference between cortical and medullary oxygenation, and thus a less steep slope. On theoretical grounds, the R2* slope can therefore be seen as a marker of cortico-medullary differentiation. It also provides a parameter that can be compared between subjects, different centres and possibly even different field strengths. Of note, the slope factor is less observer-independent than the R2* curve. This is most likely explained by the fact that the slope is directly influenced by the manual placement of the inner border. Further improvement is therefore needed. Ideally, the placement of the inner border should not rely on the human eye but become an observer-independent, automatic procedure.

Another limitation of the TLCO technique remains its inability to differentiate between cortex and medulla. Integration of the R2* response to furosemide into the algorithm, and blood flow-based MRI techniques such as arterial spin labelling, could potentially help to overcome this shortcoming in the future. Finally, the absolute thickness of the renal parenchyma is not integrated in the analysis, so between-layer differences are relative and cannot be easily translated into changes in R2* values per mm of renal tissue parenchyma.

In conclusion, the TLCO technique is an observer-independent method to analyse BOLD-MRI images. This technique provides detailed layer-by-layer information on the R2* values and hence on the level of oxygenation within the kidneys and a way to measure any drug-induced changes in that

oxygenation. As such, a higher R2* value (indicating hypoxia) was found in the cortical layers of CKD patients. The furosemide-induced decrease in R2* was smaller as compared with controls and hypertensive persons, indicating a reduced renal response to furosemide in CKD. The TLCO technique also provides the unique opportunity to calculate a new parameter—the slope factor—that does not solely rely on mean R2* values, but merely on intra-renal geometrical distribution and change. This slope factor may be an indirect index of the cortico-medullary differentiation, though this conjecture needs validation in biopsy studies. Whether this slope factor has prognostic potential and adds valuable information to the prediction of renal function decline on top of classical risk markers will also need further study.

SUPPLEMENTARY DATA

Supplementary data are available online at http://ndt.oxfordjournals.org.

ACKNOWLEDGEMENTS

This study was supported by a grant from the Swiss National Science Foundation (FN 32003B-149309) and by the Centre d'Imagerie BioMédicale (CIBM) of the University of Lausanne (UNIL).

CONFLICT OF INTEREST STATEMENT

None declared. The results presented in this paper have not been published previously in whole or part, except in abstract format.

REFERENCES

1. Ponte B, Pruijm M, Marques-Vidal P *et al.* Determinants and burden of chronic kidney disease in the population-based CoLaus study: a cross-sectional analysis. *Nephrol Dial Transplant* 2013; 28: 2329–2339
2. Fine LG, Norman JT. Chronic hypoxia as a mechanism of progression of chronic kidney diseases: from hypothesis to novel therapeutics. *Kidney Int* 2008; 74: 867–872
3. Haase V. Hypoxia-inducible factor signaling in the development of kidney fibrosis. *Fibrogenesis Tissue Repair* 2012; 5: S16
4. Manotham K, Tanaka T, Matsumoto M *et al.* Evidence of tubular hypoxia in the early phase in the remnant kidney model. *J Am Soc Nephrol* 2004; 15: 1277–1288
5. Prasad PV. Evaluation of intra-renal oxygenation by BOLD MRI. *Nephron Clin Pract* 2006; 103: c58–c65
6. Pruijm M, Hofmann L, Vogt B *et al.* Renal tissue oxygenation in essential hypertension and chronic kidney disease. *Int J Hypertens* 2013; 2013: 696598
7. Pruijm M, Hofmann L, Piskunowicz M *et al.* Determinants of renal tissue oxygenation as measured with BOLD-MRI in chronic kidney disease and hypertension in humans. *PLoS One* 2014; 9: e95895
8. Michaely HJ, Metzger L, Haneder S *et al.* Renal BOLD-MRI does not reflect renal function in chronic kidney disease. *Kidney Int* 2012; 81: 684–689
9. Vink EE, de Boer A, Hoogduin HJ *et al.* Renal BOLD-MRI relates to kidney function and activity of the renin-angiotensin-aldosterone system in hypertensive patients. *J Hypertens* 2015; 33: 597–603; discussion 603–604
10. Prasad PV, Thacker J, Li LP *et al.* Multi-parametric evaluation of chronic kidney disease by MRI: a preliminary cross-sectional study. *PLoS One* 2015; 10: e0139661
11. Prasad PV, Edelman RR, Epstein FH. Noninvasive evaluation of intrarenal oxygenation with BOLD MRI. *Circulation* 1996; 94: 3271–3275
12. Li LP, Ji L, Santos E *et al.* Effect of nitric oxide synthase inhibition on intrarenal oxygenation as evaluated by blood oxygenation level-dependent magnetic resonance imaging. *Invest Radiol* 2009; 44: 67–73
13. Simon-Zoula SC, Hofmann L, Giger A *et al.* Non-invasive monitoring of renal oxygenation using BOLD-MRI: a reproducibility study. *NMR Biomed* 2006; 19: 84–89
14. Pedersen M, Dissing TH, Morkenborg J *et al.* Validation of quantitative BOLD MRI measurements in kidney: application to unilateral ureteral obstruction. *Kidney Int* 2005; 67: 2305–2312
15. Piskunowicz M, Hofmann L, Zuercher E *et al.* A new technique with high reproducibility to estimate renal oxygenation using BOLD-MRI in chronic kidney disease. *Magn Reson Imaging* 2015; 33: 253–261
16. Levey AS, Eckardt KU, Tsukamoto Y *et al.* Definition and classification of chronic kidney disease: a position statement from Kidney Disease: Improving Global Outcomes (KDIGO). *Kidney Int* 2005; 67: 2089–2100
17. Saad A, Crane J, Glockner JF *et al.* Human renovascular disease: estimating fractional tissue hypoxia to analyze blood oxygen level-dependent MR. *Radiology* 2013; 268: 770–778
18. Ebrahimi B, Gloviczki M, Woollard JR *et al.* Compartmental analysis of renal BOLD MRI data: introduction and validation. *Invest Radiol* 2012; 47: 175–182
19. Thacker JM, Li LP, Li W *et al.* Renal blood oxygenation level-dependent magnetic resonance imaging: a sensitive and objective analysis. *Invest Radiol* 2015; 50: 821–827
20. Vakilzadeh N, Phan O, Ogna VF *et al.* New aspects of hypertension management in patients with chronic kidney disease. *Rev Med Suisse* 2014; 10: 1668–1672
21. Epstein FH, Prasad P. Effects of furosemide on medullary oxygenation in younger and older subjects. *Kidney Int* 2000; 57: 2080–2083
22. Prasad PV, Epstein FH. Changes in renal medullary pO2 during water diuresis as evaluated by blood oxygenation level-dependent magnetic resonance imaging: effects of aging and cyclooxygenase inhibition. *Kidney Int* 1999; 55: 294–298
23. Pruijm M, Hofmann L, Maillard M *et al.* Effect of sodium loading/depletion on renal oxygenation in young normotensive and hypertensive men. *Hypertension* 2010; 55: 1116–1122
24. Pohlmann A, Arakelyan K, Hentschel J *et al.* Detailing the relation between renal T2* and renal tissue pO2 using an integrated approach of parametric magnetic resonance imaging and invasive physiological measurements. *Invest Radiol* 2014; 49: 547–560
25. Tanaka T, Kato H, Kojima I *et al.* Hypoxia and expression of hypoxia-inducible factor in the aging kidney. *J Gerontol A Biol Sci Med Sci* 2006; 61: 795–805
26. dos Santos EA, Li LP, Ji L *et al.* Early changes with diabetes in renal medullary hemodynamics as evaluated by fiberoptic probes and BOLD magnetic resonance imaging. *Invest Radiol* 2007; 42: 157–162

Received: 26.5.2016; Editorial decision: 18.8.2016

ORIGINAL ARTICLE